27th International Conference on Flexible Automation and Intelligent Manufacturing, FAIM2017, 27-30 June 2017, Modena, Italy

Effect of coefficient of thermal expansion (CTE) mismatch of solder joint materials in photovoltaic (PV) modules operating in elevated temperature climate on the joint's damage

Osarumen O. Ogbomo[a*], Emeka H. Amalu[b], N.N. Ekere[a], P. O. Olagbegi[c]

[a]*School of Engineering, Faculty of Science and Engineering, University of Wolverhampton, WV1 1LY, UK*
[b]*Department of Mechanical, Aerospace and Civil Engineering, School of Science and Engineering, Teesside University, Middlesbrough, Tees Valley, TS1 3BA, UK*

[c]*Mechanical Engineering Department, Faculty of Engineering, University of Benin, Nigeria*

[*]*Email Address: O.O.Ogbomo@wlv.ac.uk, ogbomoosarumen@yahoo.com; Tel.: +44(0)7471372448*

Abstract

With failure of solder joints (SJs) in photovoltaic (PV) modules constituting over 40% of the total module failures, investigation of SJ's reliability factors is critical. This study employs the Garofalo creep model in ANSYS Finite Element Modelling (FEM) to simulate solder joint damage. Accumulated creep strain energy density is used to quantify damage. PV modules consisting of interconnections formed from different material combinations (silver, copper, aluminum, zinc, tin and brass) are subjected to induced temperature cycles ranging from -40 °C to +85 °C. Results show that zinc-solder-silver joint having the highest CTE mismatch of 19.6 ppm exhibits the greatest damage while silver-solder-silver with no mismatch possesses the least damage.

Peer-review under responsibility of the scientific committee of the 27th International Conference on Flexible Automation and Intelligent Manufacturing.

Keywords: Photovoltaic modules; Solder interconnections; Solder joint damage; Garofalo creep model; Thermal cycling; Accelerated damage; Elevated temperature climates; Coefficient of thermal expansion; Relative expansion mismatch

1. Introduction

Photovoltaic (PV) modules are designed to operate under standard test conditions (STCs) [1]–[3]. These STCs are solar radiation of 1000 W/m², cell temperature of 25 °C, wind speed of 1 m/s and air mass (AM) of 1.5. The actual operating conditions differ from the STCs and vary from climate to climate [4]–[8]. Field failures of PV modules include delamination and discolouration of EVA, solder bond and ribbon degradation and cracking as well as burn marks. Kato Kazuhiko [9] amongst other researchers have reported solder interconnection damage as responsible for over 40% of PV Module failures[10]–[13] and hence the focus of this study.

Peer-review under responsibility of the scientific committee of the 27th International Conference on Flexible Automation and Intelligent Manufacturing.

PV modules are comprised of different materials with distinctive properties some of which are presented in Tables 1 & 2. Figure 1 shows a typical crystalline PV module with two PV cells connected in series by solder interconnections. The failure of PV modules operating in elevated temperature climates is caused by the accelerated degradation of solder joint interconnections. During operation, the different materials which make up the solder interconnections expand and contract at different rates (i.e. relative expansion rates) which imply a mismatch in their coefficients of thermal expansions (CTEs). This CTE mismatch of the bonded materials in the solder joint is responsible for the thermo-mechanical induced deformation of the PV module.

This study seeks to investigate the effect of CTE mismatch of the bonded materials in the solder joint on the damage of PV modules operating in elevated temperature climates. This will provide useful information which can be used to increase the static-structural reliability of PV module interconnection with regards to the choice of materials bonded together in the assembly.

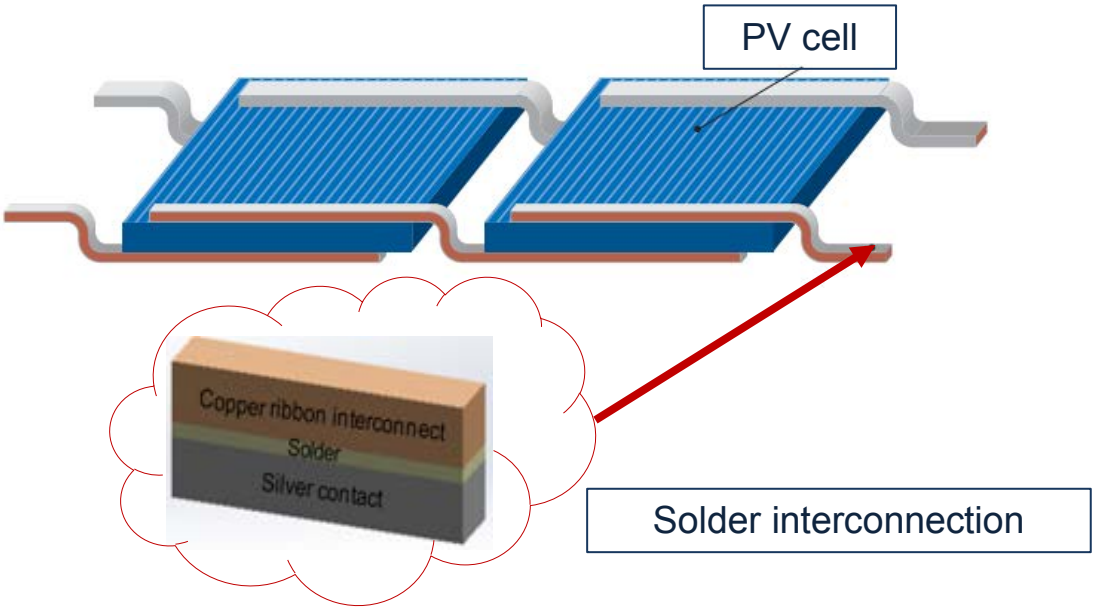

Figure 1: Typical crystalline PV module[15]

2. Thermal load

The designed models of the PV module were subjected to temperature load utilizing International Electro-technical Commission (IEC) 61215 standard to simulate thermal stresses on the materials of the models [16]. The thermal load ranged from -40 °C to +85 °C for six thermal cycles. The derived temperature profile is presented in Figure 2.

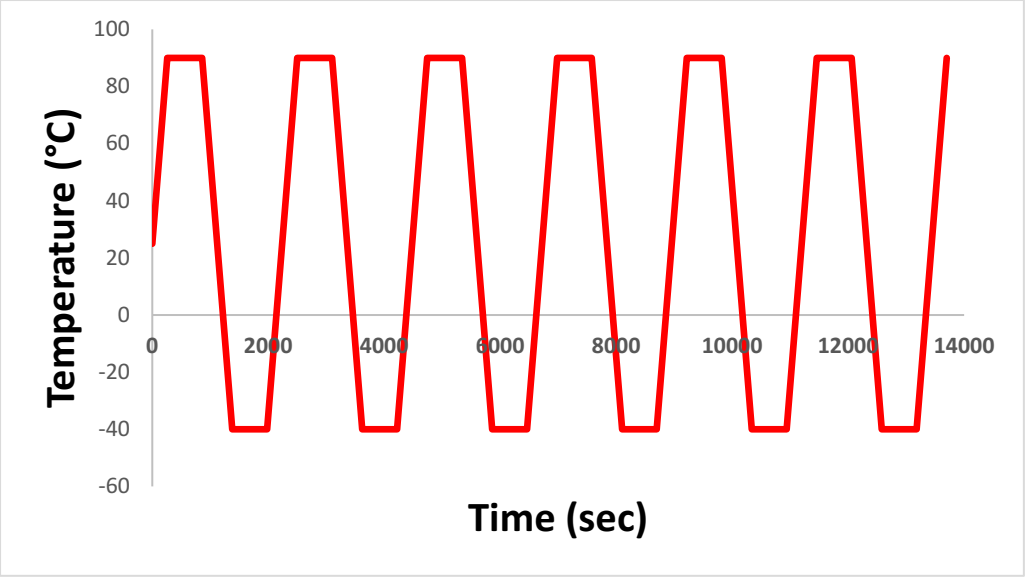

Figure 2: Induced temperature cycle load ranging from –40°C to +85°C

3. Finite element analysis

Finite element modelling (FEM) was employed to investigate the effect of CTE mismatch of bonded materials in solder joint on the damage of PV modules operating in elevated temperature climates. The modelling is presented in three subsections. Model and Methodology presented in sub section 3.1, Materials and their properties in 3.2 and Finite Element Modelling in 3.3.

3.1. Model and methodology

PV solder interconnections typically comprise of copper ribbons joined to silver contacts by Sn3.5Ag0.5Cu solder alloy. For the purpose of this study, the solder and silver contact materials and thickness were kept constant while the ribbon interconnect material was varied. Materials used for the ribbon interconnect are silver, copper, aluminum, zinc, tin and brass. These materials and their respective properties are found in Tables 1 and 2. The PV module was modelled using Solid Works software and then simulated with ANSYS Mechanical software to generate accumulated creep strain energy density used to quantify solder joint damage.

Garofalo creep model (equation 1) was used to simulate the damage response of solder while other material responses were modelled using appropriate models. For each material combination, the creep strain energy is measured using ANSYS Mechanical. Figure 5 shows the creep strain energy distribution for the copper-solder-silver solder joint.

$$\varepsilon_{cr} = C_1[\sinh(C_2\sigma)^{C_3} \exp C_4 /T] \quad \textbf{(1)}$$

Where, ε_{cr}= creep strain rate,C_1,C_2, C_3, C_4 = Garofalo creep parameters for SnAgCu solder (presented in Table 3), σ= Equivalent Von Mises Stress and T= absolute temperature.

3.2. Materials and their properties

The PV module materials and their properties are presented in Table 1 and presented in Figures 3 & 4. The solder interconnection materials are presented in Table 2. Material properties shown include CTE, Young's Modulus and Poisson Ratio. Table 3 presents the Garofalo creep constants employed to model the solder interconnection damage for the respective material combinations. Garofalo creep model was used to determine the accumulated creep strain energy density which is the measure of solder joint damage. Further discussions on creep strain energy density are carried out in section 4.

Table 1: PV Module materials and respective properties

Material	Coefficient of Thermal Expansion (CTE) (10^{-6}/K^{-1})	Young's Modulus (GPa)	Poisson Ratio	Thermal Conductivity (W/mK)	Shear Modulus (GPa)
Glass	**8.5**	**73.3**	**0.21**	**1.8**	**30.289**
EVA	**270**	**0.011**	**0.4999**	**0.35**	**0.00367**

Table 2: Solder Interconnection Materials and respective properties

				399	**31.978**
Solder	**23.2**	**43**	**0.30**	**60**	**16.5**
Silver	**10.4**	**7**	**0.37**	**429**	**2.5547**
Silicon	**3.5**	**130**	**0.22**	**148**	**53.279**
Aluminium	**11.9**	**6**	**0.33**	**237**	**2.2556**

Table 2: Solder interconnection materials and respective properties

			4	**0.2**	**0.5**

Material	Coefficient of Thermal Expansion (CTE) (10^{-6}/K^{-1})	Young's Modulus (GPa)	Poisson Ratio	Thermal Conductivity (W/mK)
Silver	**20**	**83**	**0.37**	**429**
Copper	**17**	**129**	**0.34**	**399**
Aluminum	**23**	**70**	**0.35**	**237**
Zinc	**30**	**108**	**0.25**	**115**
Brass	**19**	**125**	**0.31**	**109**
Tin	**23.4**	**50**	**0.36**	**66**
Solder	**23.2**	**43**	**0.30**	**60**

Table 3: Garofalo creep parameter values for SnAgCu solder [14]

Parameter	**C_1 (s^{-1})**	**C_2 $(MPa)^{-1}$**	**C_3**	**C_4 (K)**
Value	277984	0.02447	6.41	6500

3.3. Finite element model

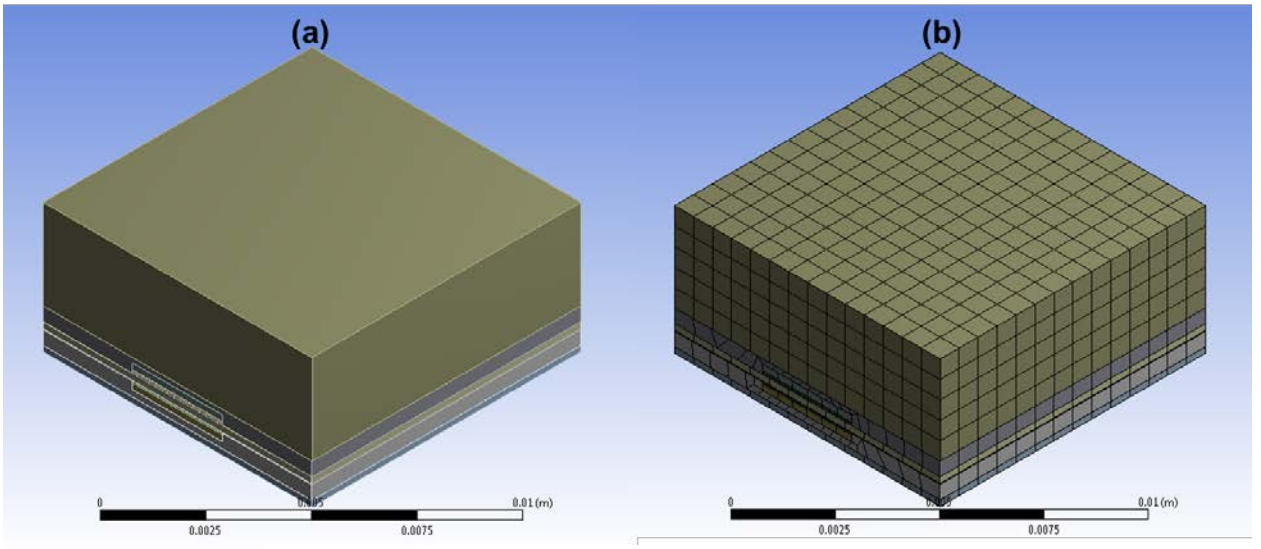

Figure 3: PV module 3D view (a) showing default mesh (b)

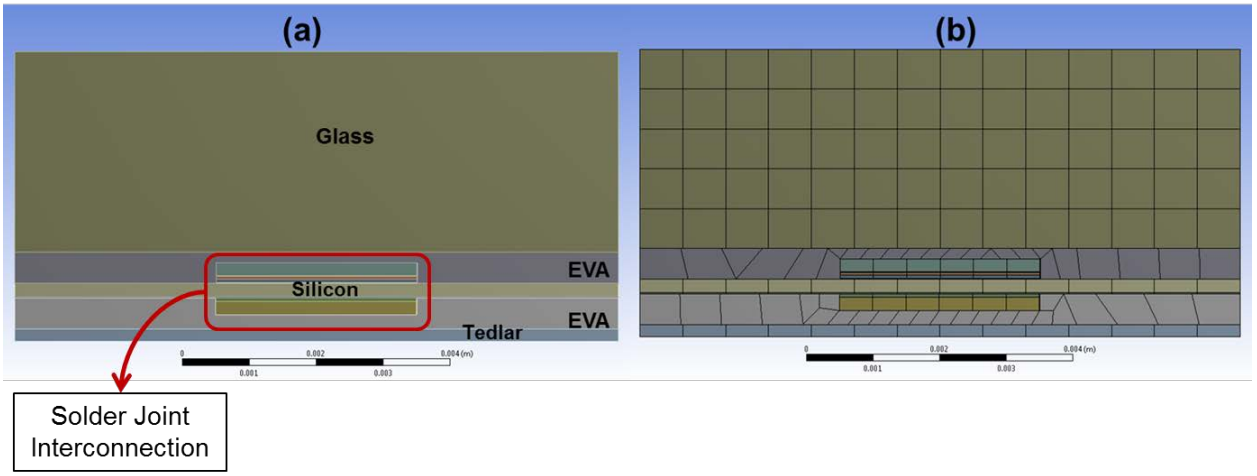

Figure 4: PV module end view (a) showing default mesh (b)

4. Results and discussion

Figure 5 shows the creep strain energy density (solder damage) of the copper-solder-silver solder interconnection. The colours signify degree of solder damage with red as greatest and dark blue as least degree of solder damage. Table 4 presents the various bonded material combinations and their respective solder joint damage. The zinc-solder-silver joint with highest CTE mismatch of 19.6 ppm exhibits the greatest damage while the silver-solder-silver joint with no CTE mismatch demonstrated the least damage. These results are also represented in Figure 6. As for now, no direct correlation is observed between CTE mismatch of bonded materials in PV interconnections and solder joint damage. However, it is clear that material combinations with little or no CTE mismatch possess less solder joint damage

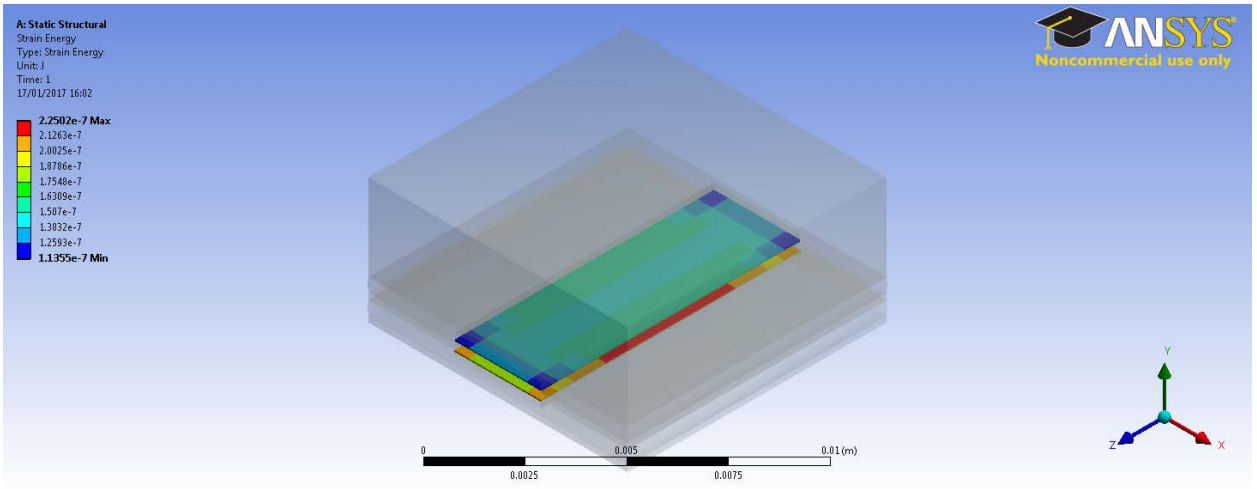

Figure 5: Creep Strain Energy Density (Solder damage) of the copper-solder-silver solder joint

Table 4: Material combinations and respective solder joint damages

Material combination	CTE mismatch (ppm)	Solder joint damage (Pascal)
Copper/Silver	6.6	6.11
Aluminium/Silver	12.6	6.00
Zinc/Silver	19.6	6.21
Tin/Silver	13	5.89
Brass/Silver	8.6	6.19
Silver/Silver	0	4.64

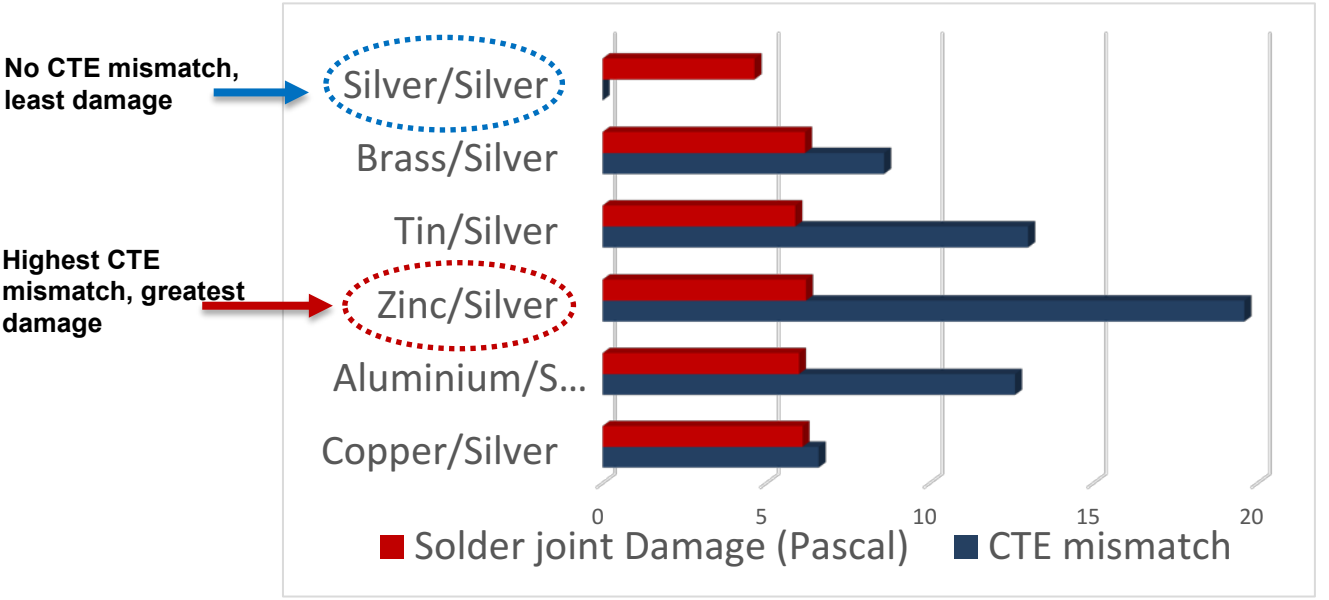

Figure 6: Material combinations and respective solder joint damages

5. Conclusion

A study on the effect of CTE mismatch of bonded materials in solder joint interconnection on the damage of PV modules solder joints operating in elevated temperature climates was carried out using ANSYS FEM. The interconnections of the PV module were formed from different material combinations. The material and thickness of solder and contact materials are kept constant while the ribbon interconnect material was varied i.e. silver, copper, brass, aluminium, tin and zinc. Accumulated creep strain energy density; the measure of solder joint damage was measured under induced temperature load ranging from -40 °C to +85 °C for 6 cycles.

The zinc-solder-silver joint with highest CTE mismatch of 19.6 ppm exhibits the greatest damage while the silver-solder-silver joint with no CTE mismatch demonstrated the least damage. These findings provide useful information that can be used to improve the static-structural reliability of PV module interconnections with regards to the choice of materials bonded together in the assembly.

Acknowledgements

The authors acknowledge the Schlumberger Faculty for the Future Foundation for providing the funding for the research reported in parts in this article. They are grateful to the staff of the University of Wolverhampton for their support/assistance and also to the University of Benin, Nigeria for providing some field data on PV module operations.

References

[1] O. O. Ogbomo, E. H. Amalu, N. N. Ekere, and P. O. Olagbegi, "A review of photovoltaic module technologies for increased performance in tropical climate," 2016.

[2] A. Skoczek, T. Sample, and E. D. Dunlop, "The results of performance measurements of field-aged crystalline silicon PV modules," *Prog. Photvoltaics Res. Appl.*, 2009.

[3] M. A. Green, "Crystalline and thin-film silicon solar cells: state of the art and future potential," *Sol. Energy*, vol. 74, no. 3, pp. 181–192, 2003.

[4] W. Sinke, "Wafer - based silicon PV technology Status , innovations and outlook."

[5] A. Ndiaye, A. Charki, A. Kobi, C. M. F. Kébé, P. A. Ndiaye, and V. Sambou, "Degradations of silicon photovoltaic modules: A literature review," *Sol. Energy*, vol. 96, pp. 140–151, 2013.

[6] A. Al Tarabsheh, S. Voutetakis, A. I. Papadopoulos, P. Seferlis, I. Etier, and O. Saraereh, "Investigation of temperature effects in efficiency improvement of non-uniformly cooled photovoltaic cells," *Chem. Eng. Trans.*, vol. 35, no. 2009, pp. 1387–1392, 2013.

[7] M. D. Kempe and J. H. Wohlgemuth, "Evaluation of Temperature and Humidity on PV Module Component Degradation," *IEEE 39th Photovoltaics Spec. Conf.*, vol. 39, pp. 120–125, 2013.

[8] E. Skoplaki and J. a. Palyvos, "Operating temperature of photovoltaic modules: A survey of pertinent correlations," *Renew. Energy*, vol. 34, no. 1, pp. 23–29, 2009.

[9] K. Kato, "PV module failures observed in the field - solder bond and bypass diode failures -."

[10] N. Park, J. Jeong, and C. Han, "Estimation of the degradation rate of multi-crystalline silicon photovoltaic module under thermal cycling stress," *Microelectron. Reliab.*, vol. 54, no. 8, pp. 1562–1566, 2014.

[11] J.-S. Jeong, N. Park, and C. Han, "Field failure mechanism study of solder interconnection for crystalline silicon photovoltaic module," *Microelectron. Reliab.*, vol. 52, no. 9–10, pp. 2326–2330, Sep. 2012.

[12] M. T. Zarmai, N. N. Ekere, C. F. Oduoza, and E. H. Amalu, "A review of interconnection technologies for improved crystalline silicon solar cell photovoltaic module assembly," *Appl. Energy*, vol. 154, no. SEPTEMBER, pp. 173–182, 2015.

[13] J. Kim, J. Park, D. Kim, and N. Park, "Study on Mitigation Method of Solder Corrosion for Crystalline Silicon Photovoltaic Modules," *Int. J. Photoenergy*, vol. 2014, pp. 13–17, 2014.

[14] A. Syed, "Accumulated creep strain and energy density based thermal fatigue life prediction models for SnAgCu solder joints," *2004 Proceedings. 54th Electron. Components Technol. Conf. (IEEE Cat. No.04CH37546)*, vol. 1, pp. 737–746, 2004.

[15] K. Y. Robert Kaminski, "Ultra Flexible Copper." NEOMAX MATERIALS Co. LTD, 2014.

[16] IEC, "Basic Understanding of IEC Standard for Testing Photovoltaic Panels" *The Compliance Information Resource for Electrical Engineers*, 2010.